Dynamic simulation of milling operations with small diameter milling cutters: effect of material heterogeneity on the cutting force model

Edouard Rivière-Lorphèvre, Christophe Letot, François Ducobu, Pierre Dehombreux & Enrico Filippi

Meccanica
An International Journal of Theoretical and Applied Mechanics AIMETA

ISSN 0025-6455

Meccanica
DOI 10.1007/s11012-016-0398-y

Meccanica
DOI 10.1007/s11012-016-0398-y

Dynamic simulation of milling operations with small diameter milling cutters: effect of material heterogeneity on the cutting force model

Edouard Rivière-Lorphèvre · Christophe Letot · François Ducobu · Pierre Dehombreux · Enrico Filippi

Received: 18 September 2015 / Accepted: 18 February 2016

Abstract Simulation of manufacturing processes (also called virtual manufacturing) is an important research topic in order to optimize the added value of the manufacturing chain. The mastering of these techniques allows companies to remain competitive on the market. Machining operations are very complex to simulate numerically due to the severe conditions undergone by the material (high strain, very high strain rates, high temperature,...). In addition, the rising need of micro-manufacturing techniques creates new challenges in numerical simulation. Indeed, some physical phenomena neglected for traditional machining simulation need to be taken into account for accurate simulation when the feedrate is fairly low (size effect, minimum chip thickness, material heterogeneity,...). New developments are thus needed to unlock the full benefits of these techniques. The aim of this paper is to enhance the classical mechanistic cutting force model for milling operations with small diameter tool by considering the effect of the heterogeneity of the material. The variability of the response during a test on fixed conditions (cutting tool, machined material and cutting parameters) is taken into account to develop a model whose parameters can evolve during a given operation. The statistical dispersion of cutting forces observed during experimental test is measured and modeled as a random perturbation of the force. The effects of this perturbation on the stability of milling operations are then demonstrated by means of numerical simulation.

Keywords Machining · Numerical simulation · Statistical analysis

E. Rivière-Lorphèvre (✉) · C. Letot · F. Ducobu · P. Dehombreux · E. Filippi
Machine Design and Production Engineering Laboratory, Faculty of Engineering (FPMs), University of Mons (UMONS), 20 Place du Parc, 7000 Mons, Belgium
e-mail: edouard.riviere@umons.ac.be

1 Introduction

Many industrial sectors are currently facing the challenge of miniaturization. This trend leads to an increasing demand for micro-components. Several micro-manufacturing techniques have been developed and improved for this purpose. One of them is micro-milling that consists in a micro-machining process using a cutting tool (having a typical diameter between 100 and 500 μm) rotating at high speed to remove material from the workpiece and producing parts and features between some mm and some μm [1–4]. Micro-milling is considered to be one of the most flexible and fastest way to produce complex tridimensional microshapes, including sharp edges, with a good surface quality in many materials such as metal alloys, composites, polymers and ceramics [5]. Even if such miniaturization is not needed, precise generation of small dimension details may be necessary for

Published online: 25 February 2016

industrial parts. The use of smaller tools with reduced cutting parameters (depth of cut or feed per tooth) is not just the downsizing of traditional milling. Some phenomena that can be neglected on traditional machining can have a significant impact such as the nonlinear rise of the specific cutting forces at small chip thickness (called 'size effect') or the minimum chip thickness leading to no chip formed at small feed [6, 7]. Another consequence of the downsizing is the fact that the workpiece material cannot be considered as homogeneous anymore (Fig. 1), so the cutting force value can be fairly different from one point to another [8, 9].

In order to reduce the production costs, simulation of manufacturing techniques has an increasing role for industrial application. These simulation tools (often referred as 'virtual manufacturing') are useful to reduce setup procedure by limiting the number of trials and errors necessary to find optimal operational parameters. Some manufacturing processes already use reliable methods for production testcases [10] but machining often break the numerical chain [11].

Machining operation simulation has to face several problems linked to complex material behavior (high strain, very strain rate and high temperature of the material), complex geometry of tools and/or part and dynamic modeling issues. In addition, it has been thoroughly observed that experimental results in machining do not give constant output for a given set of experimental parameters (small variation of cutter geometry, cutting parameters, surface roughness or composition of workpiece). Currently simulation is not able to model all industrial testcases so, some approximation should be used. One interesting approach is the use of mechanistic models based on numerical analysis coupled with experimental tests [12–14].

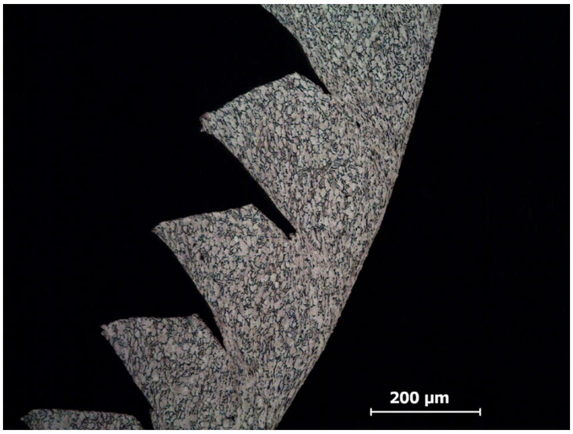

Fig. 1 Ti6Al4V chip machined at a cutting speed of 30 m/min and undeformed chip thickness of 280 μm (*lighter color* is the α phase, *darker* is the *β* phase)

The aim of this paper is to adapt an inverse analysis method to retrieve numerical model of cutting force during machining operation with a small diameter mill. The variability of the signal linked to the heterogeneity of the material is taken into account from a statistical point of view and its effect on stability is observed. The general methodology is described in [15], this paper extends the analysis to a series of measured data to demonstrate that the results obtained remains consistent when the cutting conditions are changed. The analysis allows the definition of cutting force model parameters valid for a broad range of cutting parameters. Finally, the addition of a random perturbation (identified from the variability of the measured signal) on the model is performed in order to be closer to the experimental results. The effects of these elements on the stability of a milling operation is then numerically observed.

2 Experimental investigation of cutting forces

2.1 Modeling approach

Two main approaches are generally used for machining simulation: meso-scale simulation and macro-scale simulation. These methods are complementary and have their own advantages and drawbacks:

– mesoscopic approach tends to simulate physical phenomena happening during chip formation. In addition to cutting forces, several other aspects can be studied such as chip morphology, temperature, surface integrity or tool wear [16, 17]. These models are often limited to simple geometries (abundant literature is dedicated on 2D orthogonal cutting) due to the intensive computation time required;
– macroscopic models use simple analytic laws to model machining process interactions. Several models for orthogonal cutting have been used in the literature [18] (linear relation between chip section and forces, exponential model, model

taking friction of the chip on cutting edge into account, ...) and generalization to oblique cutting has also been performed [19]. These models are easier to compute, so more complex geometries can be used to solve coupled problems (stability and chatter vibrations, form error, ...). These models are anyway more limited because experimental test must be performed to get the actual values of the parameters of the model.

This research uses a macroscopic approach and is focused on the modeling of the behavior on a plane perpendicular to the axis of the cutter (the force acting along the cutter is usually neglected on stability analysis).

In the macroscopic simulation of the milling process, the most common approach to simulate the cutting forces along the complex shape of a cutter is to divide the tool into infinitesimal slices along cutter axis [19]. On each of these slices, the elementary cutting forces are computed on three orthogonal directions (t along the cutting speed, r along the local normal to the cutter and a orthogonal to r and t) using simple analytic laws depending on macroscopic quantities (depth of cut, undeformed chip thickness,...). For this paper, simple linear model has been used as shown in Eq. 1

$$\begin{aligned} \mathrm{d}F_t &= K_t \cdot h \cdot db \\ \mathrm{d}F_r &= K_r \cdot h \cdot db \\ \mathrm{d}F_a &= K_a \cdot h \cdot db \end{aligned} \qquad (1)$$

Coefficient K_t, K_r and K_a are the specific pressure, h is the undeformed chip thickness (computed using kinematic model as presented in [20]) and db is the height of the slice. The geometric description of cutter with complex shape has been performed in [21] so all elementary efforts can be projected on a global frame and then analytically integrated along the cutting edges to obtain the total effort.

2.2 Experimental setup

The experimental tests were performed on a Witech 628 micro-milling machine (Fig. 2). The cutting forces during machining were measured with a Kistler dynamometer (Type 9256C2) at a sampling frequency of 71428 Hz. A series of shoulders ($a_e = 1$ mm, $a_p = 2$ mm) have been machined on a Ti6Al4V titanium block precisely machined before the experimental campaign to ensure constant depth of cut during the tests. A 2 mm diameter carbide tool with two teeth (SECO 512020Z2.0-SIRON-A) has been used. In order to avoid the effects of tool wear, each mill has been changed after less than five minutes of cutting. Experimental tests were carried out using cutting speeds ranging from 60 to 90 m/min and feed ranging from 8 to 12 µm per tooth following tool supplier specifications. Each cutting condition was repeated twice to check repeatability (a summary of the tests is proposed on Table 1). In order to illustrate the adjustment process, the first test of the experimental plan is selected and will be used for Figs. 3, 4 and 5. The programmed cutting speed is 75 m/min, the feed per tooth is 10 µm/tooth. Figure 3 shows the measured signal in this case.

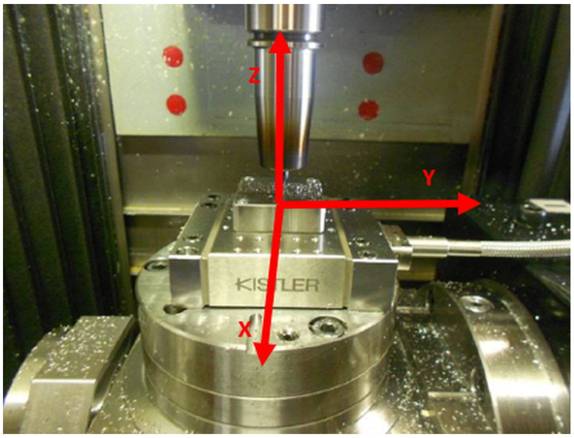

Fig. 2 Picture of the experimental setup

The measured signal has been filtered with a low-pass Butterworth filter at a frequency of 2 kHz (the bandwidth of the dynamometer is around 4 kHz). The first numerical treatment on the measured signal consist in the evaluation of the root mean square (RMS) difference between the force signal at each revolution of the tool. Several spindle speeds close to the programmed one are tested.

The measured signal is thus resampled at a frequency which is a multiple of the estimated spindle frequency to perform the computation using cubic spline interpolation. Root mean square criterion is used to estimate the agreement between consecutive tool revolutions:

Table 1 Summary of the results obtained with all experimental tests

Test	V_c (m/min)	f (µm/tooth)	K_t (MPa)	K_r (MPa)	$rms_x(N)$	$rms_y(N)$	$\sigma_{\%x}$ (%)	$\sigma_{\%y}$ (%)	ρ_x^2	ρ_y^2
1.1	60	8	2916	2342	3.32	3.90	1.36	2.11	97.2	97.9
1.2			2946	2380	3.32	4.40	1.25	1.86	97.6	98.6
2.1		9	2776	2151	3.40	4.23	1.13	1.66	97.9	98.5
2.2			2835	2198	3.36	4.50	1.09	1.54	97.8	98.1
3.1		10	2691	2024	3.39	4.68	1.15	1.77	97.7	98.2
3.2			2713	2059	3.47	4.89	1.15	1.70	97.8	98.4
4.1		11	2592	1920	3.52	5.03	1.11	1.79	98.2	98.5
4.2			2609	1938	3.60	5.17	1.12	1.85	97.7	98.5
5.1		12	2524	1831	3.55	5.36	1.09	1.48	95.8	98.3
5.2			2556	1837	3.32	5.58	1.06	1.73	97.7	98.5
6.1	75	8	2770	2310	3.33	4.58	1.09	1.60	97.3	98.4
6.2			2747	2339	3.64	4.55	0.99	1.42	97.4	98.4
7.1		9	2627	2127	3.84	4.85	1.27	1.83	97.2	97.8
7.2			2653	2142	3.53	4.89	1.19	1.68	97.4	98.2
8.1		10	2512	1922	4.06	5.13	1.23	1.61	97.6	98.7
8.2			2477	1960	4.02	5.11	1.15	1.74	97.4	98.5
9.1		11	2445	1846	3.87	5.59	1.04	1.35	97.5	98.5
9.2			2415	1873	4.15	5.54	1.03	1.32	97.5	98.7
10.1		12	2362	1749	3.86	5.70	1.24	1.66	95.5	97.9
10.2			2345	1768	4.27	5.71	1.07	1.53	96.7	98.2
11.1	90	8	2597	2248	3.59	3.84	1.34	1.70	97.7	98.1
11.2			2669	2248	3.45	4.04	1.26	1.55	97.2	98.2
12.1		9	2504	2054	3.78	4.34	1.33	1.92	97.1	98.0
12.2			2543	2087	3.86	4.53	1.19	1.53	97.5	98.6
13.1		10	2448	1948	3.85	4.51	1.29	1.65	97.7	98.1
13.2			2447	1945	4.08	4.90	1.02	1.40	98.4	98.8
14.1		11	2409	1812	3.66	4.73	1.27	1.58	97.5	98.4
14.2			2365	1830	4.20	5.19	1.10	1.29	98.2	98.9
15.1		12	2326	1705	4.13	5.23	1.28	1.60	96.5	98.0
15.2			2346	1732	4.02	5.40	1.10	1.33	97.2	98.7

V_c is the cutting speed, f the feed per tooth, *rms* the root mean square difference between measured and simulated signal without perturbation, K_t and K_r the specific pressures, $\sigma\%$ the ratio of mean standard deviation obtained during the variability analysis by the peak force, ρ^2 the coefficient of determination obtained by the variability analysis

$$RMS_i = \sqrt{\frac{1}{n}\sum_{j=1}^{n}\left(F_{i,j} - \overline{F_i}\right)^2}, \qquad \overline{F_i} = \frac{1}{n}\sum_{j=1}^{n} F_{i,j} \tag{2}$$

i is the direction of the force (x,y or z), j is the sampled position of the test (n samples during one cutting test).

The spindle speed value with the lower RMS is kept as the best estimator of the actual spindle speed. This analysis has two main purposes:

- retrieve the actual spindle speed during the experimental test that can be slightly different from the programmed speed (the knowledge of this value is crucial for an accurate determination of specific pressure);
- the knowledge of this speed allows to work on the mean force over only one revolution of the tool in order to lower the computing time for the inverse analysis (the result would be quite similar to the whole recorded signal but it would require the use

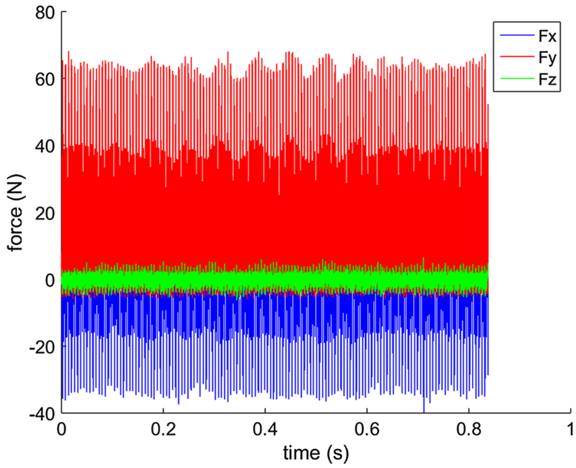

Fig. 3 Experimental recording at a cutting speed of 75 m/min and a feed of 10 μm/tooth recording

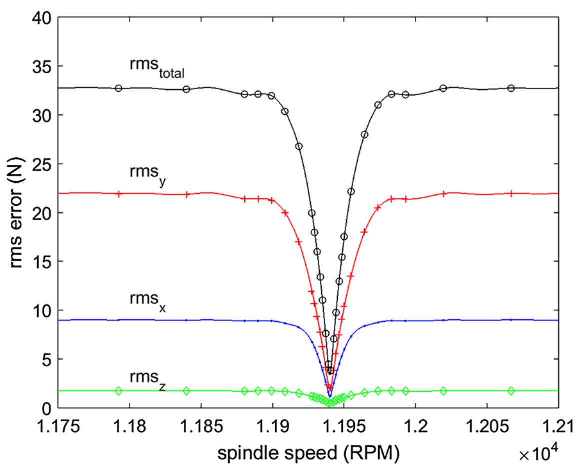

Fig. 4 Evolution of rms value as a function of estimated spindle speed for the 75 m/min and 10 μm/tooth recording

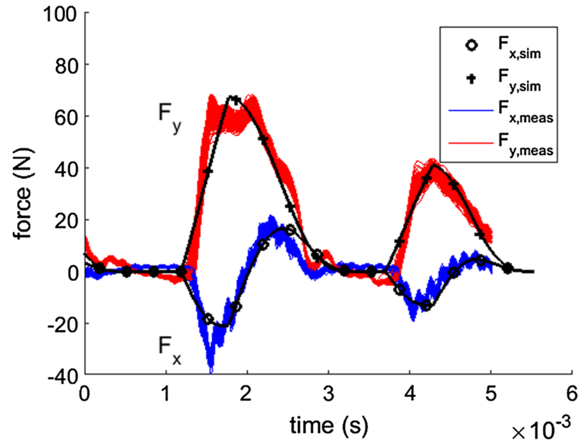

Fig. 5 Simulated signal superimposed with measured cutting forces for all revolutions of the tool testcase 75 m/min and 10 μm/tooth recording

of higher dimension matrix thus higher computation time).

The evolution of the RMS value with respect to the estimated spindle speed for the sample measurement is shown in Fig. 4. The minimum is at 11,940 RPM (to be compared with the programmed speed of 11,936 RPM).

2.3 Inverse analysis

The parameters of analytic models are not easily retrievable from mechanical properties of the materials. Several authors developed methods to retrieve these parameters from experimental measurement [22–24]. The approach used in this paper is based on the fitting of analytic model on temporal measurement of cutting forces measured during machining. This model allows the identification of parameters for linear or nonlinear analytic laws and is also able to estimate run-out of the cutter during experiments [20].

The main idea is to convert the cutting force computation in a matrix relationship. For local cutting force (Eq. 1), we can write:

$$\begin{Bmatrix} \mathrm{d}F_t \\ \mathrm{d}F_r \\ \mathrm{d}F_a \end{Bmatrix} = \overbrace{\begin{bmatrix} h \cdot db & 0 & 0 \\ 0 & h \cdot db & 0 \\ 0 & 0 & h \cdot db \end{bmatrix}}^{[A]} \cdot \overbrace{\begin{Bmatrix} K_t \\ K_r \\ K_a \end{Bmatrix}}^{\{K\}} \tag{3}$$

The elementary efforts are then projected in the reference frame of the dynamometer. The classical transformation matrix performs the projection.

$$\begin{Bmatrix} \mathrm{d}F_x \\ \mathrm{d}F_y \\ \mathrm{d}F_z \end{Bmatrix} = [B] \cdot \begin{Bmatrix} \mathrm{d}F_t \\ \mathrm{d}F_r \\ \mathrm{d}F_a \end{Bmatrix} \tag{4}$$

$$[B] = \begin{bmatrix} -\cos\phi & -\sin\phi \cdot \sin\kappa & -\sin\phi \cdot \cos\kappa \\ \sin\phi & -\cos\phi \cdot \sin\kappa & -\cos\phi \cdot \cos\kappa \\ 0 & -\cos\kappa & -\sin\kappa \end{bmatrix} \tag{5}$$

ϕ is the angle describing the revolution around the axis of the tool, κ is the orientation of the normal vector with respect to the cutter axis. The undeformed chip thickness can be computed with a kinematic model taking radial runout into account [20].

These relationships are then added for each tooth and each disc to perform numerical integration along the cutting edges:

$$\begin{Bmatrix} F_x \\ F_y \\ F_z \end{Bmatrix} = \sum_{i=1}^{n_d} \sum_{j=1}^{n_t} \begin{Bmatrix} dF_x(i,j) \\ dF_y(i,j) \\ dF_z(i,j) \end{Bmatrix} = \overbrace{\left(\sum_{i=1}^{nd} \sum_{j=1}^{nt} [B] \cdot [A] \right)}^{[C]} \cdot \{K\} \tag{6}$$

Matrix C (dimension 3 $\times$ 3) links cutting coefficients to cutting forces. At each time step a matrix $[C^k]$ can be build (k is the index of the current time step). All these matrix are then assembled to get the global system:

$$\overbrace{\begin{Bmatrix} \begin{bmatrix} F_x^1 \\ F_y^1 \\ F_z^1 \end{bmatrix} \\ \begin{bmatrix} F_x^2 \\ F_y^2 \\ F_z^2 \end{bmatrix} \\ \vdots \end{Bmatrix}}^{[F]} = \overbrace{\begin{bmatrix} \boxed{C^1} \\ \boxed{C^2} \\ \vdots \end{bmatrix}}^{[D]} \cdot \{K\} \tag{7}$$

The specific pressure can be computed by filling the vector $\{F\}$ with the measured forces and by applying least square optimization method to solve the overdetermined system:

$$[K] = \left([D]^{\mathrm{T}}[D]\right)^{-1} \cdot \left([D]^{\mathrm{T}}[F]\right) \tag{8}$$

$[K]$ is the matrix containing specific pressure, $[D]$, the assembly of all $[C^k]$ matrix and $[F]$ the measured cutting forces.

All the parameters having a nonlinear effect on the model are obtained by optimization routine. The quality criteria is again the RMS between measured and simulated signals.

Figure 5 shows the superimposition of the simulated signal with the identified specific pressure and the measured signal for each revolution of the tool (as mentioned earlier, the only values used for stability analysis will be on the plane perpendicular to the spindle axis, so figures will only show efforts along x and y directions). The identified parameters are $K_t = 2512$ MPa, $K_r = 1922$ MPa and a runout of 2.2 µm.

Although the machining is stable, it can be observed that the values of the efforts are varying from one revolution to another. This trend is similar for all the machining tests that were performed. Several possible causes of variability have been minimized during the experimental procedure (precise machining of the blanks used for the tests to avoid variation of the depth of cut, use of simple trajectories during the tests to avoid dynamic change of the feedrate,...) so the main cause of variation lies in the material itself. Titanium alloy Ti6Al4V is a two-phased material with alpha and beta grain with different material properties that can lead to local modifications of the cutting force (depending on the phase of the grain being machined). The hypothesis of this paper is that this is the main source of variability on the system. The formation of serrated chip while machining titanium alloy could be another source of variation, but this phenomenon arises at a frequency that is a higher than the range of interest of the experimental tests (segmentation frequency above 5 kHz is observed in [25, 26] for example). Section 3 will describe the proposed method to take this effect into account.

2.4 Global analysis

In order to model wider range of operation with the same model, a design of experiment (DOE) approach has been achieved to model the specific pressure for the different cutting parameters of the experimental data [27]. The summarized model is given by:

$$K_{t,MPa} = 2689 \cdot \left(\frac{V_c}{V_{c0}}\right)^{-0.239} \cdot \left(\frac{S_t}{S_{t0}}\right)^{-0.349} \tag{9}$$

$$K_{r,MPa} = 2044 \cdot \left(\frac{V_c}{V_{c0}}\right)^{-0.133} \cdot \left(\frac{S_t}{S_{t0}}\right)^{-0.656} \tag{10}$$

$V_{c0} =$ m/min and $S_{t0} = 10$ µm/tooth are reference values of cutting speed and feed per tooth. The coefficient of determination ρ^2 is used to assess the quality of the adjustment:

$$\rho^2 = 1 - \frac{\sum_i (K_i - k_i)^2}{\sum_i \left(K_i - \overline{K}\right)^2} \tag{11}$$

with K_i the ith computed value, $\overline{K}$ the mean of computed values and K_i the ith modeled value. The coefficient of determination ρ^2 is over 95 % for both models (98.1 % for K_t and 99.5 % for K_r) so the correlation is strong (Figs. 6, 7)

3 Uncertainty management

As it can be seen from the experimental results, the cutting forces recorded during the experimental tests present some fluctuations for each revolution of the cutter. As far as most sources of perturbation has been minimized, the hypothesis is that this variability is linked to the heterogeneity of the machined material. This perturbation can affect the stability of the milling process [28, 29] this section describes a method to add this effect on the cutting force model.

An approach is to treat the variation of the cutting forces around its mean value as a random signal whose parameters can be identified. For each sample time, a normal distribution was fitted on the recorded force values, each adjustment was achieved on 90 values (90 consecutive revolutions of the tool are selected on the measured file). The adjustment of the normal law distribution was performed by using a regression method, based on the median rank estimator to obtain a non-parametric cumulative density function ($\widehat{CDF}$) of the measured cutting forces for each sample time [30]:

$$\widehat{CDF}(F_i) = \frac{i - 0.3}{N + 0.4} \tag{12}$$

with i being the index of the ith measured cutting force F_i sorted by ascendant values and N the number of points considered in the distribution. The cumulative density function of the normal distribution is:

$$CDF(F) = \Phi\left(\frac{F - \mu}{\sigma}\right), \tag{13}$$

with $\Phi(x)$ the standard normal distribution ($\mu = 0$, $\sigma = 1$) given by:

$$\Phi(x) = \frac{1}{\sqrt{2\pi}} \int_{-\infty}^{x} \exp\left(-\frac{F^2}{2}\right) \tag{14}$$

The inverse function takes the form:

$$\Phi^{-1}[CDF(F)] = -\frac{\mu}{\sigma} + \frac{1}{\sigma} F \tag{15}$$

which results in a linear equation with slope parameter $1/\sigma$ and constant parameter $-\mu/\sigma$. Using the discrete data $[F_i, \widehat{CDF}(F_i)]$ from Eq. 12 in Eq. 15 allows to find the parameters μ and σ by regression using a probability plot. The Table 1 shows the main results of the fitting procedure, the ratio of standard deviation over peak force is fairly constant for all the experimental test. The mean value of 1.16 % for x and 1.62 % for y will be considered for the rest of the paper.

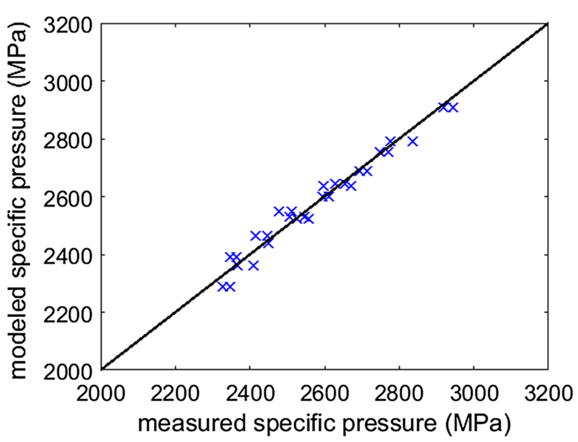

Fig. 6 Comparison between measured and modeled coefficient K_t

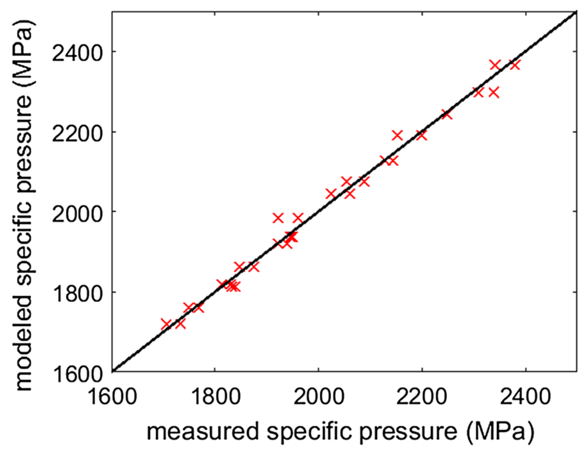

Fig. 7 Comparison between measured and modeled coefficient K_r

4 Stability of milling operation

4.1 Modification of the cutting force model

In order to take the variability of the cutting force signal into account, a random noise can be superimposed on the simulated signal. The estimated mean standard deviations obtained for force signal along the three directions (see Sect. 3) were used to obtain the same type of signal as the measured one. Figure 8 shows an example of simulated signal for the same cutting conditions as Fig. 5. It can be observed that the range of variation of the efforts is similar. In addition, the analysis proposed on Sect. 3 has been performed on the simulated signal to ensure that the uncertainty parameters have been correctly taken into account.

4.2 Stability lobes computation

This proposed model has been tested for dynamic simulation of milling operation. In order to show the effect of variability of the cutting force on the stability of the operations, both cutting forces models (mean signal and signal with random component) have been used to predict stability lobes. The proposed system has the dynamic parameters of a micro-milling machine found in [31] (first eigenfrequency at 4035 Hz, damping of 1.6 %). The same tool is used (2 mm diameter, 2 flutes) and the parameters of cutting forces model are those identified earlier. The stability lobes are obtained classical methods

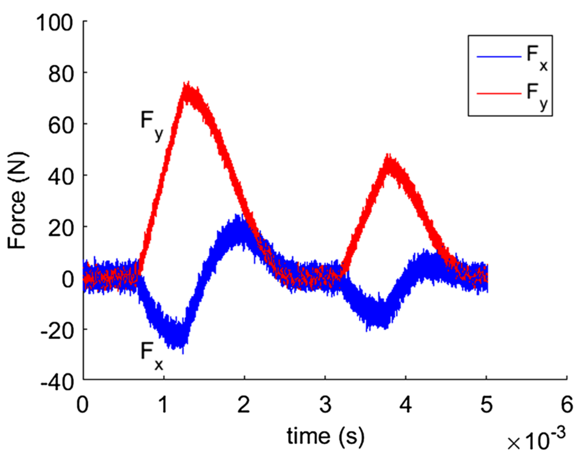

Fig. 8 Simulation of the cutting force taking variability into account

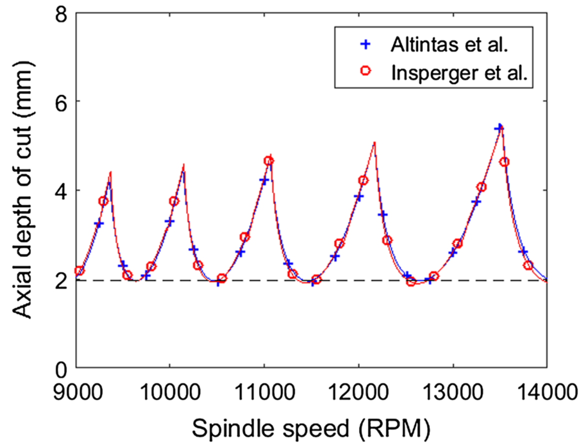

Fig. 9 Stability lobes using linear method or semi-discretization

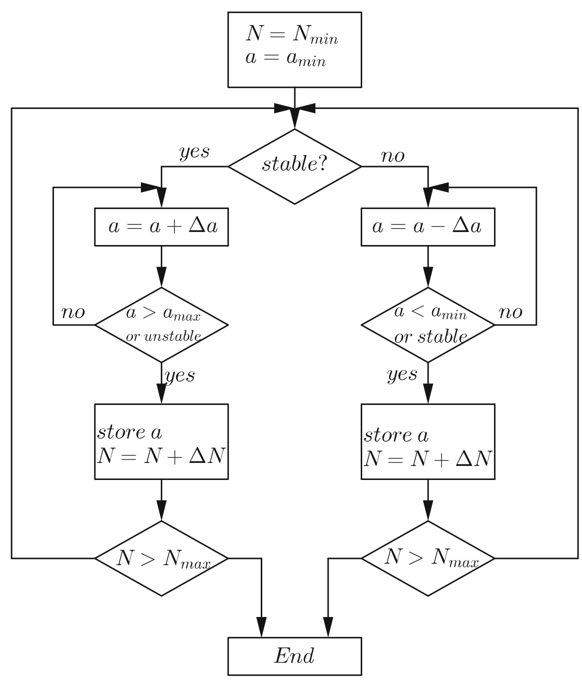

Fig. 10 Algorithm used to determine stability lobes using dynamic simulations (*a* axial depth of cut, *N* spindle speed)

proposed in the literature (linear method [32] or semi-discretization [33]) as shown in Fig. 9) and also by performing full dynamic simulation of milling at different spindle speeds and axial depths of cut. The classical algorithm used to determine the stability lobes in this case is shown in Fig. 10. The limit depth of cut (that separates stable and unstable regions) is

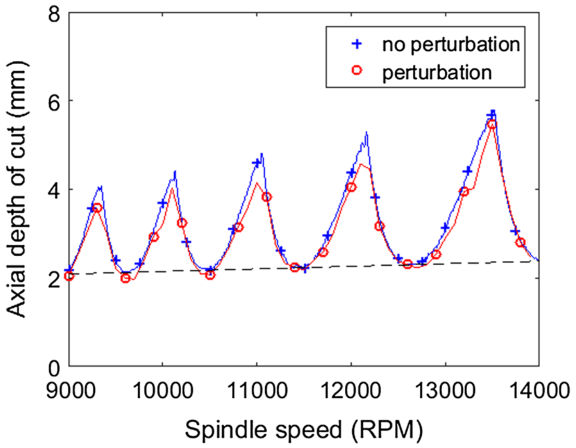

Fig. 11 Stability lobes computed with dynamic simulation using the cutting force model previously identified (with and without the effect of heterogeneity)

selected as the one showing an increase of 25 % of undeformed chip thickness as compared to the rigid case (this method has been proposed in [34]). Stability lobes diagram obtained by dynamic analysis is shown on Fig. 11. The comparison with the stability lobes obtained with classical approach shows that the general trend is the same: the position of the maximum peaks are located at the same frequencies and the order of magnitude of the limit axial depth of cut is similar. However, the use of the identified cutting forces model shows a variation of the unconditional limit of stability (minimum of all lobes) due to the variation of specific pressure with respect to cutting speed. The lobes obtained with the model taking variability into account have lower stability limit. The limit axial depth between stable and unstable operation decrease of a mean value of 5 %. The difference depends on the spindle speed and goes up to 15 % at 13,300 RPM.

5 Conclusion

In this paper a numerical and experimental analysis of the cutting forces produced by a milling operation with a small diameter cutter is performed. The generalization of an inverse analysis method for cutting forces simulation has been achieved on a series of experiments where the sources of variability have been minimized (except the heterogeneity of the workpiece material).

First the measured signal has been used to compute the exact spindle speed using the auto-correlation of the signal along each cutter revolution. Then the mean value has been used to retrieve the best analytic cutting force coefficients. An analysis of variability of the signal has been performed in order to add the effect of unpredictable variation during machining (claimed to be linked to the heterogeneity of the material). Finally, this variable model has been applied on dynamic simulation of milling operation to compute stability lobes.

The simulations show that the variability of the cutting force leads to a decrease of stability of the system.

Acknowledgments The authors would like to acknowledge competence center 'Technocampus' in Gosselies (Belgium) for their help during the experimental tests and the provision of their machine tools.

Appendix: complete results

See Table 1.

References

1. Chae J, Park S, Freiheit T (2006) Investigation of micro-cutting operations. Int J Mach Tools Manuf 45:313–332
2. Dornfeld D, Min S, Takeuchi Y (2006) Recent advances in mechanical micromachining. Ann CIRP 55:745–768
3. Liu X, DeVor R, Kapoor S, Ehman K (2004) The mechanics of machining at the micro scale: assessment of the current state of the science. J Manuf Sci Eng 126:666–678
4. Camara MA, Campos Rubio JC, Abrao AM, Davim JP (2012) State of the art on micromilling of materials, a review. J Mater Sci Technol 28(8):673–685
5. Weule H, Huntrup V, Trischler H (2001) Micro-cutting of steel to meet new requirements in miniaturization. Ann CIRP 50:61–64
6. Ducobu F, Rivière-Lorphèvre E, Filippi E (2011) A lagrangian fem model to produce saw-toothed macro-chip and to study the depth of cut influence on its formation in orthogonal cutting of ti6al4v. Adv Mater Res 223:1–11
7. de Oliveira FB, Rodriguez AR, Coelho RT, de Souza AF (2015) Size effect and minimum chip thickness in micromilling. Int J Mach Tools Manuf 89:39–54
8. Ljustina G, Larsson R, Mn Fagerstrom (2014) A fe based machining simulation methodology accounting for cast iron microstructure. Finite Elem Anal Des 80:1–10
9. Simoneau A, Ng E, Elbestawi MA (2006) The effect of microstructure on chip formation and surface defects in

micro-scale, mesoscale, and macroscale cutting of steel. Ann CIRP 55:97–102

10. Altan T, Vazquez V (1997) Numerical process simulation for tool and process design in bulk metal forming (keynote paper). Ann CIRP 45(2):599–615
11. Brecher C, Esser M, Witt S (2009) Interaction of manufacturing process and machine tool. CIRP Ann Manuf Technol 58:588–607
12. Thepsonthi T, Özel T (2012) Multi-objective process optimization for micro-end milling of ti-6al- 4v titanium alloy. Int J Adv Manuf Technol 63:903–914
13. Thepsonthi T, Özel T (2013) Experimental and finite element simulation based investigations on micro-milling ti-6al-4v titanium alloy: effects of cbn coating on tool wear. J Mater Process Technol 213:532–542
14. Pratap T, Patra K, Dyakonov AA (2015) Modeling cutting force in micro-milling of ti-6al-4v titanium alloy. Proc Eng 129:134–139
15. Rivière-Lorphèvre E, Letot C, Ducobu F, Filippi E (2015) Uncertainty management of cutting forces parameters and its effects on machining stability. Key Eng Mater 651–653:1165–1170
16. Attanasio A, Ceretti E, Rizzuti S, Umbrello D, Micari F (2008) 3d Finite element analysis of tool wear in machining. CIRP Ann Manuf Technol 57:61–64
17. Axinte DA, Dewes RC (2002) Tool wear and workpiece surface integrity when high speed ball nose end milling hardened AISI h13. In: Metal cutting and high speed machining. Kluwer Academic/ Plenum publishers, pp 171–179
18. Denkena B, Hollman F (2013) Process machine interactions: prediction and manipulation of interactions between manufacturing processes and machine tool structure. Springer lecture notes in production engineering
19. Altintas Y (2000) Manufacturing automation, metal cutting. Cambridge university press, New York
20. Rivière-Lorphèvre E, Filippi E (2009) Mechanistic cutting force model parameters evaluation in milling taking cutter radial runout into account. Int J Adv Manuf Technol 45(8):8–15
21. Engin S, Altintas Y (2001) Mechanics and dynamics of general milling cutters. Part I. Int J Mach Tools Manuf 41:2195–2212
22. Kline WA, DeVor RE, Lindberg JR (1982) The prediction of cutting forces in end milling with application to cornering cuts. Int J Mach Tool Des Res 22:7–22
23. Budak E, Altinta Y, Armarego EJA (1996) Prediction of milling force coefficients from orthogonal cutting data. ASME J Manuf Sci Eng 118:216–224
24. Ko JH, Cho DW (2005) Detremination of cutting-condition-independent coefficients and runout parameters in ball-end milling. Int J Adv Manuf Technol 26:1211–1221
25. Sun S, Brandt M, Dargusch M (2009) Characteristics of cutting forces and chip formation in machining of titanium alloys. Int J Mach Tools Manuf 49:561–568
26. Ducobu F, Rivière-Lorphèvre E, Filippi E (2014) Numerical contribution to the comprehension of saw-toothed ti-6al-4v chip formation in orthogonal cutting. Int J Mech Sci 81:77–87
27. Rivière-Lorphèvre E, Filippi E, Dehombreux P (2011) Experimental investigation of parameter-dependent analytical cutting force models for the simulation of the milling process. In: Proceeding of ESAFORM2011
28. Schmitz TL, Karandikar J, Kim NH, Abbas A (2011) Uncertainty in machining: workshop summary and contributions. J Manuf Sci Eng 133(5):051009
29. Duncan GS, Kurdi M, Schmitz T (2005) Stability lobe uncertainty. In: Proceedings of American society for precision engineering annual meeting
30. Wasserman G (2002) Reliability verification, testing and analysis in engineering design. CRC Press, Boca Raton
31. Afazov SM, Ratchev SM, Segal J, Popov AA (2012) Chatter modelling in micro-milling by considering process nonlinearities. Int J Mach Tools Manuf 56:28–38
32. Altintas Y, Budak E (1995) Analytical prediction of stability lobes in milling. Ann CIRP 44:357–362
33. Insperger T, Mann BP, Stepan G, Bayly PV (2003) Stability of up-milling and down-milling, part 1: alternative analytical methods. Int J Mach Tools Manuf 43:25–34
34. Campomanes ML, Altintas Y (2003) An improved time domain simulation for dynamic milling at small radial immersion. Trans ASME 125:416–422